Neuron
Report

LTD Induction Causes Morphological Changes of Presynaptic Boutons and Reduces Their Contacts with Spines

Nadine Becker,[1] Corette J. Wierenga,[1,3] Rosalina Fonseca,[1,2,3] Tobias Bonhoeffer,[1] and U. Valentin Nägerl[1,*]
[1]Max Planck Institute of Neurobiology, Am Klopferspitz 18, 82152 München-Martinsried, Germany
[2]Present address: Gulbenkian Institute of Science, Rua da Quinta Grande 6, 2780-156 Oeiras, Portugal
[3]These authors contributed equally to this work
*Correspondence: naegerl@neuro.mpg.de
DOI 10.1016/j.neuron.2008.09.018

SUMMARY

Activity-dependent changes in the synaptic connections of the brain are thought to be important for learning and memory. Imaging techniques have enabled the examination of structural rearrangements during activity-dependent processes at the synapse. While many studies have examined structural changes of dendritic spines, little is known about structural plasticity of presynaptic boutons. We therefore examined how axonal boutons are affected during long-term depression (LTD). We used time lapse two-photon laser scanning microscopy and extracellular field recordings to monitor simultaneously synaptic morphology and activity for up to five hours in mouse organotypic hippocampal slice cultures. LTD induction dramatically increased the turnover of presynaptic boutons, while decreasing the number of putative synaptic contacts between Schaffer collateral boutons and spines of CA1 pyramidal cells. Our data indicate a substantial presynaptic contribution to activity-dependent morphological plasticity and provide opportunities for studying the molecular mechanisms of the structural remodeling of synaptic circuits.

INTRODUCTION

Experience-dependent changes in synaptic connections in the brain are thought to play a key role in learning and memory as well as the fine-tuning of neural circuits during postnatal development. A number of imaging studies in recent years have revealed a close association between activity-dependent synaptic plasticity, such as long-term potentiation (LTP) or long-term depression (LTD), and structural plasticity at individual synapses (Yuste and Bonhoeffer, 2001, 2004). For instance, it was shown that the induction of LTP in hippocampal slices leads to the growth of new spines (Engert and Bonhoeffer, 1999; Maletic-Savatic et al., 1999; Toni et al., 1999) and ultimately to the formation of new synapses (Nägerl et al., 2007). LTP induction was also shown to cause dendritic spines of potentiated synapses to increase in size (Lang et al., 2004; Matsuzaki et al., 2004). In addition, the converse effect was also demonstrated; the induction of LTD causes spines on CA1 pyramidal neurons in hippocampal slices to retract and/or shrink (Nägerl et al., 2004; Zhou et al., 2004). These and other studies support the idea that morphological changes at the level of dendritic spines provide a potential structural basis of how transient changes in synaptic strength are made long lasting.

In contrast to the plasticity of dendritic spines, activity-dependent structural plasticity at the presynaptic site has not been studied in great detail. While a number of recent studies have looked at the plasticity of presynaptic boutons in adult and developing hippocampal and cortical tissue (De Paola et al., 2003, 2006; Konur and Yuste, 2004; Deng and Dunaevsky, 2005; Umeda et al., 2005; Stettler et al., 2006), most of these studies have concentrated on plasticity under unstimulated conditions. Therefore, the behavior of presynaptic boutons under the conditions of classic plasticity paradigms known to induce synaptic plasticity is still largely unknown.

We examined whether and how presynaptic boutons are affected by the activity-dependent plasticity paradigm of LTD induction. In addition, we performed two-color two-photon time lapse imaging to visualize the structural dynamics of boutons and associated spines in hippocampal organotypic slice cultures. Since LTD-inducing low-frequency stimulation is known to lead to the retraction of dendritic spines of CA1 pyramidal neurons, we examined how boutons of CA3 axons that were in close association with these spines are affected by this paradigm. Our data show that the effect of LTD on boutons is, if anything, larger than on postsynaptic spines. Beyond the well-established role of dendritic spines in the activity-dependent modifiability of synaptic connections, our data reveal a significant presynaptic contribution.

RESULTS

Imaging Activity-Dependent Structural Plasticity of Boutons and Spines

We combined two-photon microscopy with electrophysiological recordings to investigate the structural dynamics of boutons of CA3 axons subjected to the classic plasticity paradigm of long-term depression (LTD). At the beginning, we checked the synaptic nature of the axonal varicosities we set out to study.

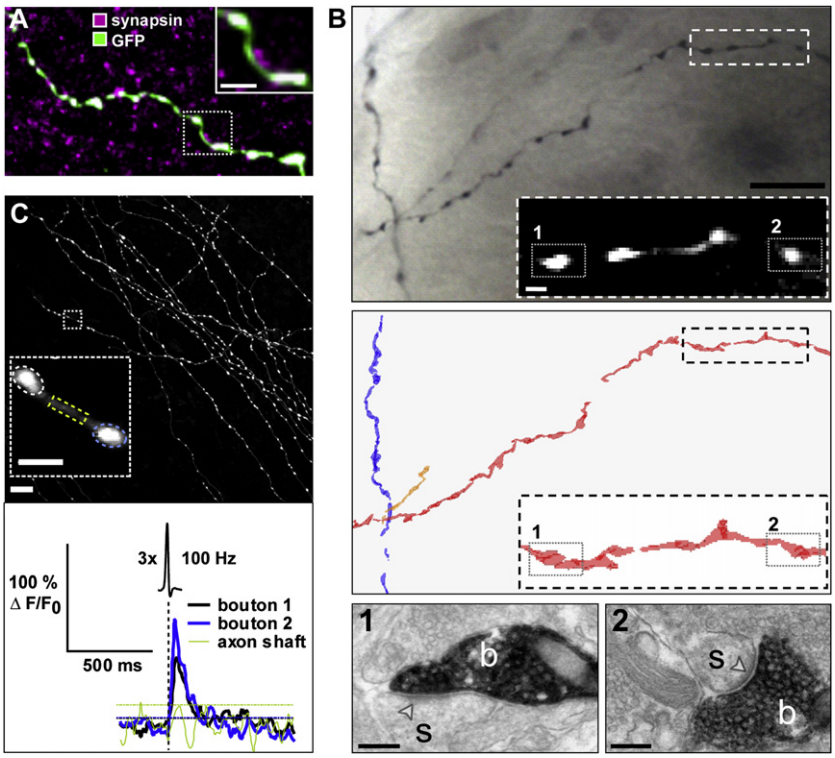

Figure 1. Axonal Varicosities Mark Functional Synapses on Schaffer Collaterals

(A) Maximal intensity projection of three subsequent confocal sections ($\Delta z = 0.5\ \mu m$) of a hippocampal slice culture, immunostained for α-synapsin displayed in magenta and for eGFP in green (overlapping pixels are white). Inset shows zoom-in on axonal stretch. Scale bar, 2 μm.

(B) Correlated light and ssEM, the upper panel shows the light microscopic image of a stretch of a labeled axon, the middle panel shows the corresponding stretch reconstructed by ssEM, and the lower two panels show EM images of two varicosities (b) that form asymmetric synapses with postsynaptic spines (s), the arrowheads marking the postsynaptic densities. Scale bars, 10 μm, 1 μm and 200 nm.

(C) Ca^{2+} imaging reveals AP-induced Ca^{2+} signals in boutons. Normalized fluorescence intensity traces; colors correspond to the regions of interest depicted in the image. Lines in respective colors indicate the 2× SD threshold.

Scale bars, 10 μm and 2 μm.

First, we examined axons by immunostainings, which revealed that the vast majority of varicosities was positive for the presynaptic marker protein synapsin (89% ± 3%, n = 191 varicosities in 6 slices), indicating that in our preparation most varicosities represent functional release sites (Figure 1A). Whether or not a varicosity was likely to be a release site did not depend on its size, since also 81% of the smallest varicosities (<0.5 μm^3) were synapsin positive. In addition, immunostainings against the vesicular glutamate transporter (VGlut1) revealed a high degree of colocalization with varicosities (80% ± 3%, n = 248 varicosities in 7 slices, data not shown), further corroborating the functional nature of the majority of axonal varicosities.

Second, we looked at the varicosities on the ultrastructural level by serial section electronmicroscopy (ssEM). To this end, we loaded individual CA3 pyramidal neurons with a fluorescent dye and biocytin permitting us to answer the question whether the varicosities are bona fide synapses. Out of a total of 23 varicosities we have examined by ssEM, 21 (91%) varicosities showed clear ultrastructural signs of synapses (as defined by the combined presence of [1] clusters of synaptic vesicles, [2] a synaptic cleft, and [3] a postsynaptic density in the apposing membrane), while for the remaining two boutons no clear evidence could be observed. Figure 1B shows single EM sections of two representative varicosities identified by light microscopy, revealing that they are part of synapses.

Third, besides the structural evidence, we wanted to check whether the varicosities would also exhibit Ca^{2+} concentration rises associated with action potential (AP) firing, which is an important criterion for their functionality. To this end, we filled individual CA3 pyramidal neurons with the Ca^{2+} indicator dye Fluo-5F via a patch pipette, which was also used to evoke APs by brief current injections. We found that AP-induced Ca^{2+} transients could readily be detected in 46 out of 47 boutons (from 15 different cells in 15 slice cultures) that were examined (Figure 1C). The Ca^{2+} transients were restricted to the immediate vicinity of the boutons, with the connecting axonal shafts showing no detectable rises in Ca^{2+} following the firing of three APs. This observation indicates that functional voltage-gated Ca^{2+} channels are enriched on the membrane of the axonal varicosities, supporting the view that axonal varicosities in our preparation indeed represent functional release sites.

LTD Induction Leads to Structural Plasticity of Presynaptic Boutons

We used low-frequency stimulation (LFS) to induce LTD at CA3–CA1 synapses (Figures 2A and 2B), which was monitored by field potential recordings in the CA1 area throughout the experiments. LFS resulted in robust LTD evidenced by a significant reduction of normalized fEPSP slopes compared to baseline (LTD, 66% ± 2%, n = 11; $p < 0.001$; Figure 2B), which is comparable with the levels of hippocampal LTD measured by extracellular recordings previously (Dudek and Bear, 1992).

To study the effects of LTD on presynaptic boutons, we quantified the number of appearing and disappearing boutons on the axons of CA3 pyramidal neurons under baseline and LTD conditions (Figures 2C–2G). LTD significantly increased the number of boutons that disappeared over 4 h of time lapse imaging after the induction compared with control conditions (boutons lost per 100 μm; LTD, 0.9 ± 0.3; n = 26 axons; control, 0.2 ± 0.1; n = 16 axons; $p < 0.05$; Figure 2G). At the same time, the rate at which new boutons appeared after LTD was also increased almost 2-fold over control conditions (boutons gained per 100 μm; LTD, 2.2 ± 0.3; n = 26 axons; control, 1.1 ± 0.2; n = 16 axons; $p < 0.01$; Figure 2G). Thus, LTD induction significantly increased the turnover rate of Schaffer collateral boutons (Table S1).

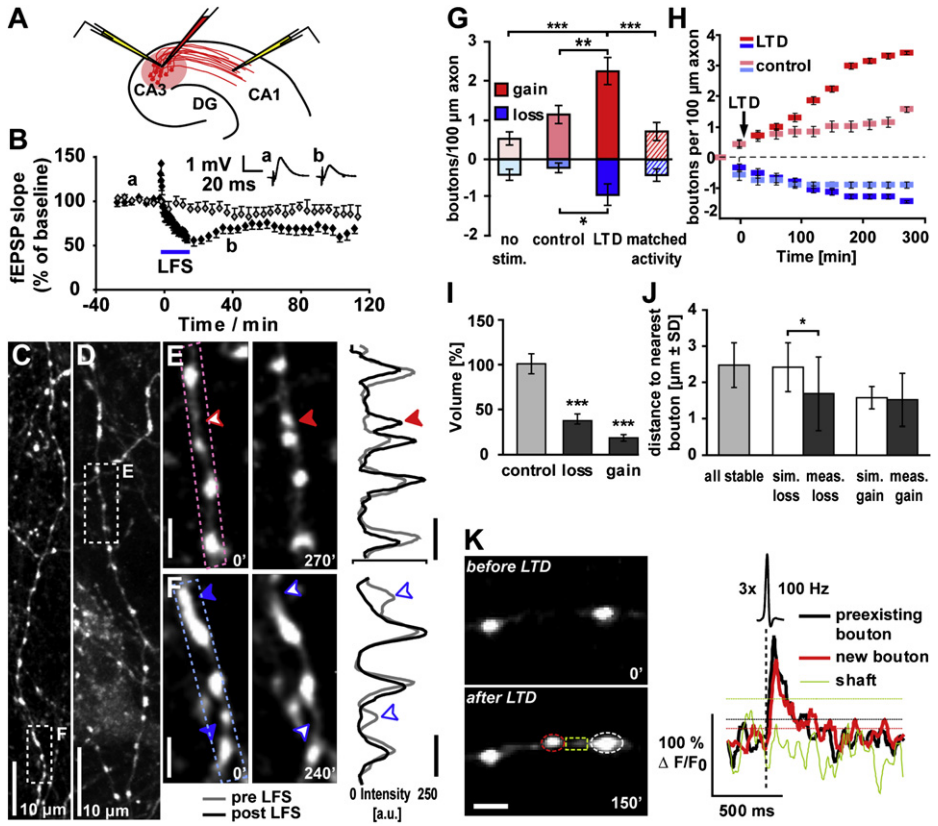

Figure 2. Structural Plasticity of Boutons after LTD Induction

(A) Schematic illustrating the experimental paradigm. Red pipette: extracellular pressure injection of Calcein red-orange AM in the CA3 area. Yellow pipettes: stimulation (left) and recording (right) electrodes after labeling was finished.

(B) Normalized and averaged fEPSP slopes (mean ± SEM) for all control (gray symbols) and LTD experiments (black symbols). Inset shows raw data traces before (a) and after (b) induction of LTD.

(C and D) Maximum intensity projections (MIPs) of labeled Schaffer collateral axons.

(E) Higher magnification of the box marked in (D) showing the emergence of a bouton (arrowhead). The graphs next to each example show the corresponding intensity plots along the parent axon before (gray) and after (black) LTD induction. Arrowheads indicate the intensity peaks of the respective boutons. Eleven sections were used for the MIPs in (C) and (D), and nine sections in (E) and (F), the Δz spacing was 0.5 µm. All scale bars 2 µm, unless otherwise indicated.

(F) Higher magnification of the box marked in (C) showing the loss of two boutons (arrowheads) after LTD induction.

(G) Summary of bouton turnover for the various experimental conditions (bouton gain in red; bouton loss in blue).

(H) Time course of bouton turnover (mean ± SEM; bouton gain in red; bouton loss in blue).

(I) Volume (mean ± SEM) of stable control boutons (gray bar), lost and gained boutons after LTD (black bars).

(J) Distance to the nearest neighboring bouton (median ± SD) for all (gray bar), simulated lost and gained (sim.; white bars), and measured lost and gained (meas.; black bars) boutons after LTD. In all panels and following figures: asterisks indicate significant differences: *$p < 0.05$; **$p < 0.01$; ***$p < 0.001$.

(K) AP-induced Ca^{2+} imaging of a new and a preexisting bouton. Normalized fluorescence intensity traces; colors correspond to the regions of interest depicted in the image. Lines in respective colors indicate the 2× SD threshold.

To test whether the morphological plasticity of boutons is specific for the LTD-inducing stimulation (LFS) or is associated more generally with elevated levels of neuronal activity, we also investigated slices with matched overall activity that did not induce LTD (see Supplemental Experimental Procedures available online) as well as unstimulated slices. We determined the turnover rate of boutons in activity-matched, control and no-stimulus conditions and found them to be statistically indistinguishable (boutons lost per 100 µm; no-stimulus, 0.4 ± 0.1; n = 14 axons; p = 0.15 compared to control; matched-activity, 0.4 ± 0.2; n = 21 axons; p = 0.36 compared to control; control, 0.2 ± 0.1; n = 16 axons; boutons gained per 100 µm; no-stimulus, 0.5 ± 0.2; n = 14 axons; p = 0.19 compared to control; matched-activity, 0.7 ± 0.2; n = 21 axons; p = 0.21 compared to control; control, 1.1 ± 0.2; n = 16 axons; Figure 2G). In addition, we analyzed two interesting experiments in which LFS failed to induce LTD, allowing us to ask the question whether the application of the LFS alone is sufficient for the structural effects we observed or whether the successful induction of synaptic plasticity is required. We found that bouton turnover in those experiments was not significantly different from control experiments (bouton turnover when LFS failed to induce LTD, n = 16 axons, bouton gain, 0.56 ± 0.15; p = 0.05 compared to control; bouton loss. 0.48 ± 0.14; p = 0.15), indicating that the enhanced turnover of presynaptic boutons is tightly linked to the expression of LTD.

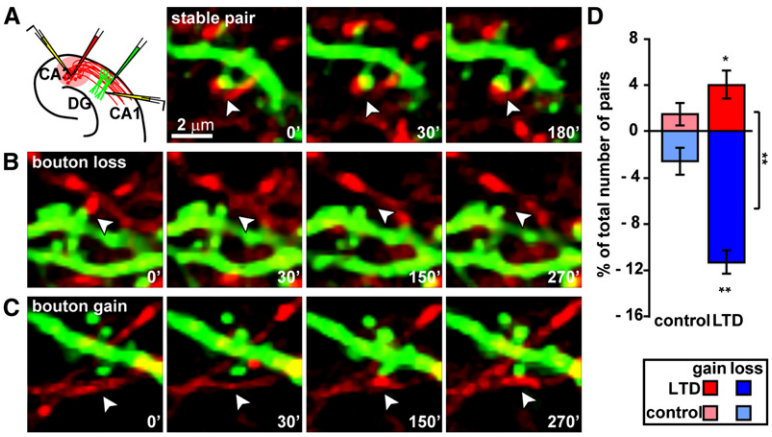

Figure 3. LTD-Induced Presynaptic Structural Plasticity in Identified Bouton-Spine Pairs

All images are single sections, chosen for best focal plane. White arrows indicate the bouton-spine pair of interest.

(A) Stable bouton-spine pair under unstimulated control conditions.

(B and C) Examples of bouton loss (B) and bouton gain (C) in bouton-spine pairs after LTD induction.

(D) Percentage of the total number of bouton-spine pairs lost (blue) or gained (red) under LTD and control conditions (mean ± SEM).

Under LTD as well as under control conditions there was a net gain of boutons over the imaging period. Of the paradigms tested only the LTD-inducing LFS reliably induced presynaptic morphological plasticity, enhancing both bouton gain and loss. The time course of the number of boutons gained or lost reveals that the onset of the increase in bouton turnover was delayed by about 2 h with respect to the start of the stimulation (Figure 2H).

In order to characterize this presynaptic structural plasticity in more detail, we measured the volume of the newly gained or lost boutons and examined their location along the axon. Boutons that appeared or disappeared after LTD (termed "plastic" boutons) were significantly smaller than stable control boutons (Figure 2I and Table S2), suggesting a higher stability for larger boutons.

We also determined for each bouton the distance to its nearest neighboring bouton. When we compared these values for plastic boutons and stable boutons, we found that nearest-neighbor distances were significantly shorter for plastic boutons (median ± SD; gained, 1.5 ± 0.8 μm, n = 24 axons, $p < 0.001$; lost, 1.7 ± 1.1 μm, n = 11 axons, $p < 0.05$; all stable, 2.5 ± 0.7 μm, n = 26 axons; Mann-Whitney U test; Figure 2J). However, if new boutons are inserted randomly between existing boutons, they are expected to have shorter nearest-neighbor distances than the existing boutons on a given axon. We therefore tested simulated random insertion and removal of boutons between the stable boutons on each axon. Based on the nearest-neighbor distance, gained boutons could not be distinguished from randomly inserted boutons (median ± SD; simulated gained, 1.6 ± 0.3 μm, n = 2600, $p = 0.84$). Lost boutons were closer to their neighbors than expected from simulated random removal (simulated lost, 2.4 ± 0.7 μm, n = 260, $p < 0.05$). This suggests that boutons disappeared preferentially if they were close to other boutons.

In order to assess the functionality of newly formed varicosities, we extended the Ca^{2+} experiments described above by imaging Ca^{2+} transients in new varicosities formed after LFS. We detected AP-induced, spatially restricted Ca^{2+} signals in all (n = 15) newly formed boutons. Interestingly, in almost all of them (14) Ca^{2+} transients could be detected as early as the first time point tested (Figure 2K), which was typically within 30 min of their initial appearance. In one of the new varicosities, Ca^{2+} transients could not be detected 30 min, but only 50 min after the new varicosity had first become visible. Taken together, the Ca^{2+} imaging data indicate that voltage-gated Ca^{2+} channels are rapidly assembled in the membranes of newly formed presynaptic structures, making it likely that they are in the process of assembling the molecular machinery needed for functional presynaptic release.

LTD-Induced Structural Plasticity in Bouton-Spine Pairs: Elevated Turnover and Net Loss of Bouton-Spine Pairs

We next examined the effect of LTD-induction on Schaffer collateral boutons that were associated with spines of CA1 pyramidal neurons. To this end, we labeled axons and dendrites by spectrally distinct dyes, allowing us to examine activity-dependent pre- and postsynaptic structural plasticity simultaneously (see Experimental Procedures for details on criteria of "contact"). While the majority of bouton-spine pairs was stably associated throughout the duration of the experiment (Figure 3A), 15% of the pairs (106 of 685) showed structural changes after LTD induction (see time course, Figure S1 available online). This corresponds to a 5-fold increase over baseline conditions (Figure 3D). Besides various pre- and/or postsynaptic structural rearrangements that caused the breakup or formation of contacts, a substantial fraction of bouton-spine pairs was lost because the bouton disappeared (33% of lost pairs; Figure 3B). In parallel, new pairs were gained by the appearance of a new bouton in contact with a spine, (50% of gained pairs; Figure 3C). The loss or gain of spines was less frequently responsible for the loss or gain of bouton-spine pairs (18% and 13%, respectively). Importantly, we never observed the retraction of a spine where the partner bouton would be "pulled" along to the dendritic shaft, suggesting that LTD does not lead to the conversion of spine synapses to shaft synapses. These results show that LTD induction also affects boutons that were associated with CA1 spines.

Presynaptic Boutons Are Affected by the Plasticity of Contacting Spines

Finally, we examined whether boutons or spines are affected if their associated partner disappears or a new partner appears. We measured the volumes of boutons and spines whose associated partner was stable, lost or gained before and after LTD. Interestingly, the volume of boutons decreased significantly after their associated spines were lost (Figures 4A–4C and Table S2),

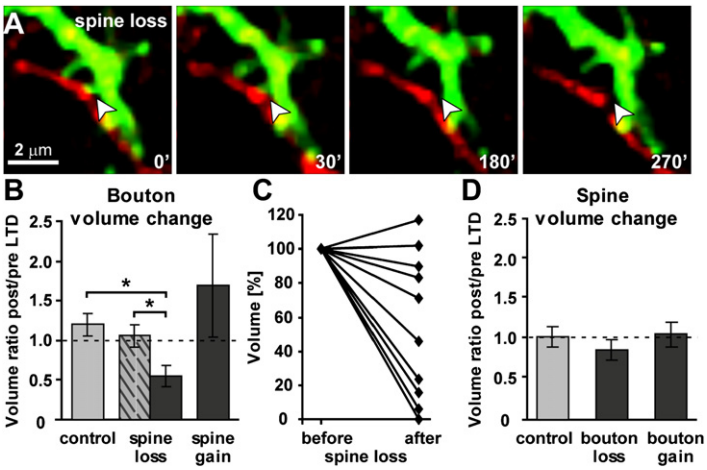

Figure 4. Characterization of the Volume Changes of Boutons Associated with Plastic Spines

(A) Example of spine loss from a bouton-spine pair.

(B) Changes in bouton volumes for stable pairs (control) and pairs in which the spine was lost or gained after LTD. Neighboring boutons that were close but not in contact with the retracting spines did not undergo any significant change in volume (striped gray bar).

(C) Volume changes shown in (B) plotted for individual boutons (n = 10).

(D) Changes in spine volumes (mean ± SEM) for stable pairs (control) and pairs in which the bouton was lost or gained after LTD.

while the volumes of boutons contacting stable spines were unaffected after LTD. Boutons right next to (but not contacting) disappearing spines had stable volumes, excluding that the reduced bouton volumes were due to unspecific regional shrinkage. The converse effect, i.e., a volume increase for boutons after coming into contact with a new spine, did not quite reach significance. In contrast to boutons, spine volume did not appear to be affected at all by the appearance or disappearance of an associated bouton (Figure 4D and Table S2).

The observation that the retraction of a spine is specifically associated with a volume reduction in the associated bouton suggests that those bouton-spine pairs had been functionally connected. Moreover, these results suggest that boutons are more affected by plastic changes of their associated partners than spines.

DISCUSSION

Our study aimed at examining activity-dependent structural plasticity from a presynaptic vantage point. We used dual-label two-photon time-lapse imaging to monitor Schaffer collateral boutons with or without contact to labeled spines of CA1 neurons in organotypic hippocampal slice cultures. First, we demonstrated that LTD induction led to a significant remodeling of presynaptic boutons, which have remained unexamined in earlier studies that focused on postsynaptic structural dynamics. Second, we showed that LTD induction reduced the number of boutons that are associated with spines, suggesting that some CA3–CA1 contacts are lost.

LTD Induces Structural Plasticity of Presynaptic Boutons

Our experiments show that the induction of LTD led to a pronounced increase (2- to 3-fold) in the turnover of presynaptic boutons. About 11% of boutons imaged during the experiment were impacted, being either gained or lost. Under control conditions, we observed a small net increase in the number of boutons, which may reflect the developmental stage of the tissue with new boutons being continuously added. The observed increased bouton gain after LTD induction seems to contrast with the net loss of contacts between boutons of CA3 axons and spines on CA1 pyramidal neurons. Given that newly formed boutons (De Paola et al., 2006) in the sensory cortex (Knott et al., 2006) can form synapses, it is likely that at least some of them ultimately will turn into functional synapses. It will be important to determine the identity of their postsynaptic partner. For instance, new boutons could form synapses with inhibitory interneurons, which would contribute to an overall decrease in synaptic transmission from CA3 to CA1. Alternatively, the new boutons could have split off from existing boutons and may be part of a dynamic pool of orphan presynaptic constituents that can be mobilized as a rapid expression mechanism of synaptic plasticity, as suggested by Krueger et al. (2003). While the presence of Ca^{2+} transients in the new boutons indicates that they may be functional, the questions of whether and when they can release neurotransmitter and form synapses awaits further study.

The fact that bouton loss takes place in close proximity to existing boutons is interesting in the light of several recent reports that neighboring presynaptic terminals can share proteins or even larger structural complexes (Krueger et al., 2003; Darcy et al., 2006; Tsuriel et al., 2006) and that this can be done in an activity-dependent fashion (Waters and Smith, 2002; Vanden Berghe and Klingauf, 2006). Together with our finding that bouton addition and removal can both occur on the same axons, this is consistent with a model in which structural elements liberated at one site during bouton removal can be used at other sites where new boutons are built.

LTD-Induced Reduction of Contacts between Schaffer Collaterals and CA1 Pyramidal Neurons

Our experiments show that LTD induction led to a considerable loss of Schaffer collateral boutons that were closely associated with CA1 spines. Although a physical contact between a bouton and a spine is necessary for a synaptic connection it is by no means sufficient. Nevertheless, several lines of evidence suggest that a significant fraction of contacts we imaged over time represented actual synapses. First, our observation that spine loss was specifically associated with a decrease in size of the corresponding bouton is suggestive of a functional contact. Second, the observation that virtually all bouton-spine pairs made contact at the spine head is consistent with EM studies that show that synapses are typically formed at the head of the spine in a one-to-one relationship between CA1 spines and boutons of Schaffer collaterals (Harris and Stevens, 1989; Schikorski and Stevens, 1997). Third, our EM data indicate that most of the morphological varicosities

along the axons represent functional presynaptic boutons. Fourth, our Ca^{2+} imaging data show that virtually all existing boutons have voltage-gated Ca^{2+} entry. This is in line with previous reports showing that almost all boutons of mature neurons are functional (Yao et al., 2006). In addition, more than 95% of all spines form synapses, at least in the neocortex (Arellano et al., 2007).

LTD induction increased the number of newly formed bouton-spine pairs by 4%, but many more pairs were lost (11%). If these contacts had been functional before they were lost, their removal may represent a structural implementation for the weakening of CA3–CA1 synaptic transmission. However, as the onset of the activity-dependent structural dynamics is delayed compared to expression of LTD, it is unlikely that contact loss plays a significant role for the early part of LTD. In any case, LTD induction appears to lead to a reorganization of pre- and postsynaptic elements, effecting a functional rewiring of the hippocampal network. This view is also supported by a recent study (Bastrikova et al., 2008) that provides evidence that LFS is associated with a reduction in bouton-spine contacts.

The percent decrease in the field responses was about twice as large as the decrease in the number of contacts, suggesting that other nonstructural LTD mechanisms, such as weakening of existing synapses without removing them, are also operational. Moreover, a discrepancy would be expected in as much as not all labeled fibers were actually stimulated, diluting the structural effect. In any case, the relationship between the number of synapses and their combined strength is likely to be highly complex, and therefore one would not expect to find a linear relationship between structural plasticity and changes in synaptic transmission. Therefore, our findings are likely to have physiological relevance, especially if the structural changes occurred within defined synaptic pathways, considering that coactivation of just a few synapses can lead to AP firing.

Our data show that structural plasticity is a feature that is not specific to dendritic spines. In fact, presynaptic structural changes may even play a bigger role than spine changes given that the gain or loss of contacts was frequently due to bouton changes. Irrespective of its mode, contact loss must entail the downregulation of cell adhesion that otherwise maintains the structural integrity of synaptic contacts (Garner et al., 2000). Understanding how LTD-induced contact loss is orchestrated at the molecular level will be an important challenge for future studies.

EXPERIMENTAL PROCEDURES

Organotypic Hippocampal Slice Cultures and Recording Solutions

Hippocampal slices (400 μm thick) were prepared from postnatal day 5–7 C57 BL/6 mice, embedded in a plasma clot on glass coverslips, and incubated in a roller incubator at 35°C, according to the Gähwiler method (Gähwiler, 1981). The slice cultures used in the experiments were maintained 10 to 17 days in vitro after the preparation. For the experiments, slice cultures were transferred into a heated recording chamber (35°C), where they were continuously perfused with carbogenated (95% O_2, 5% CO_2) artificial cerebrospinal fluid (ACSF) at pH 7.4 containing 126 mM NaCl, 2.5 mM KCl, 2.5 mM $CaCl_2$, 1.3 mM $MgCl_2$, 10 mM glucose, 1.25 mM NaH_2PO_4, 26 mM $NaHCO_3$, 1 mM pyruvate, and 1 mM trolox (Sigma, Munich, Germany).

Labeling and Microscopy

Two-color time-lapse two-photon laser scanning microscopy (TPLSM) was used to monitor the morphology of CA3 axons and spines of CA1 pyramidal neurons over time. The red excitation light (λ = 790 nm) from a 5 W Mira-Verdi laser system (Coherent, Santa Clara, CA) was routed through a laser scanhead (Yanus II, TILL Photonics, Gräfelfing, Germany), a dichroic mirror (CH-700DCXR2638; LOT Oriel, Darmstadt, Germany), and a 40×, 1.2 NA water-immersion objective (Zeiss, Oberkochen, Germany) mounted on an inverted IX70 microscope (Olympus, Hamburg, Germany). The power of the excitation light was adjusted to 2 mW after the objective by an acousto-optical modulator (Polytec, Waldbronn, Germany). The emitted fluorescence was split by a suitable dichroic mirror (HQ572LP; LOT Oriel) into red and green fluorescence, filtered by adequate band-pass filters (red channel, HQ590/55; green channel, HQ525/50; both filters from LOT Oriel), and detected by two external photomultiplier tubes (R6357, Hamamatsu, Herrsching, Germany). Image acquisition was performed by custom-programmed software (LabVIEW 8.2, National Instruments, Austin, TX).

For the structural plasticity experiments, a glass micropipette filled with 0.5 mM Calcein red-orange AM (Invitrogen, Karlsruhe, Germany) diluted in HEPES-buffered ACSF, connected to a Picospritzer (Parker Hannifin Corporation, Fairfield, NJ), was placed in the middle of the cell body layer of the CA3 area. The dye was injected into the tissue by applying brief pressure pulses of 5 to 15 ms every 20 s. After 1 hr, about 30 to 40 CA3 neurons were labeled, projecting predominantly into the stratum oriens. TPLSM was used to localize the projection area of the labeled axons of the CA3 neurons in the CA1 region. Two to four CA1 pyramidal neurons in this area were loaded for 2–3 min via a patch pipette containing 4 mM Calcein green (Invitrogen), 120 mM K-Gluconate, 10 mM KCl, 20 mM HEPES, 5 mM NaCl, and 12 mM Mg^{2+}-ATP. The field of view was chosen in the region with optimal overlap of the CA3 pyramidal cell axons and the CA1 pyramidal cell dendrites, which was always located within the stratum oriens. 3D image stacks (spanning 140 μm in x,140 μm in y, and 25–40 μm in z using 1024 × 1024 pixels in xy and 0.5 μm steps in z) were acquired every 30 min. The labeling of both sets of neurons remained constant for the duration of the experiment. For the Ca^{2+} imaging experiments, single CA3 cells were patched for up to 8 hr, the pipette containing internal solution (see above), 100 μm Fluo-5F and 200 μm Alexa Fluor 568. Eighty image frames of 5 μm × 5 μm using 64 × 64 pixels were acquired in a single, optimal z plane of one or two boutons with a frame rate of one image per 15 ms. APs were evoked after 20 frames. For the EM reconstructions of the axons, single CA3 pyramidal neurons were briefly loaded via a patch pipette with Calcein green and biocytin to produce an electron-dense label.

Electrophysiology

Field excitatory postsynaptic potentials (fEPSPs) were recorded from the cell body layer near the labeled CA1 pyramidal neurons, using a glass micropipette filled with ACSF. CA3 pyramidal neurons were stimulated by brief (0.2 ms) current pulses from a stimulus isolator (WPI, Sarasota, FL) using a glass micropipette filled with 3 M NaCl, immobilized at the tip by agar. See further details in Supplemental Experimental Procedures.

Image Analysis

4D (x, y, z, t) image stacks were processed and analyzed using ImageJ (NIH, Bethesda, MD), Imaris 5.1 (Bitplane, Zürich, Switzerland), and custom-programmed MATLAB software (Version 7.1, MathWorks, Natick, MA). Bouton turnover was analyzed blindly with respect to control and LTD experiments. Individual stacks of the red channel were visualized and filtered with a Gaussian algorithm in ImageJ. For each experiment, two to four axons were analyzed over lengths ranging from 55 to 130 μm. The selected axons were displayed and analyzed as maximum intensity projections. We assessed the presence of every bouton on the basis of intensity plots, which were calculated as the average intensity over every line of pixels from a rectangle drawn along short stretches of axon (Figures 2C and 2D). Boutons were defined by a peak intensity >30% larger than the intensity level of the axonal shaft. We used a MATLAB code to simulate the random insertion and deletion of a single bouton onto each of the axons we analyzed (100 simulated insertions and 10 simulated removals per axon). Spine turnover analysis was carried out on volume-rendered images of the green channel, which was spatially filtered by an edge-preserving algorithm using the Imaris software. In addition, individual sections were analyzed to confirm if a spine was lost or gained. All spines visible in the field of view were included in the analysis.

For the analysis of bouton-spine pairs, contacting boutons and spines were detected visually in single planes of image stacks with both channels overlaid and filtered by an edge-preserving algorithm in Imaris. We analyzed bouton-spine pairs undergoing structural changes, and a random sample of stable pairs. Only those pairs were analyzed for which both bouton and spine were centered in the same z section. The volumes of both partners of bouton-spine pairs were determined by a MATLAB program in the following manner. Stacks of raw images of both channels were read in as time series, filtered with an adaptive Wiener algorithm and drift-corrected in all dimensions. Data were binarized in each channel separately by an intensity threshold. Thresholds were empirically defined by a semiautomatic two-step procedure. In the first step, background was distinguished from neuronal structures such as dendrites and axons (threshold = mean + 3× SD of intensity values of a local 200 × 200 pixel area). In the second step, boutons were distinguished from axonal shafts (threshold = mean + 1.5× SD of axon pixel intensities). In this way, thresholds were objective and they were kept constant over all time points. Outlines of boutons and spines of putative contacts were determined semiautomatically in the individual z sections of the thresholded images of the separate channels. From these, the volumes of the individual structures were calculated.

Data are reported as means ± SEM unless stated otherwise. Statistical significance of the effects of LTD was calculated using two-tailed, unpaired t tests. Statistical significance of the effect of changing boutons or spines on their contact partner was determined using two-tailed, paired t tests. In cases of multiple comparisons, p values were post hoc Bonferroni corrected. In total, we analyzed 908 pairs of boutons and spines; of those, 223 came from 5 slices in control experiments and 685 came from 11 slices in LTD experiments.

Immunostaining

See Supplemental Experimental Procedures.

Serial Section Electronmicroscopy and 3D Reconstructions

Slices were initially transferred into 35°C 0.1 M phosphate buffer (PB)-based fixative containing 4% paraformaldehyde, 15% picric acid, and 0.5% glutaraldehyde and subsequently stored at 4°C for 4 hr on a shaker. Slices were removed from the coverslip using a paint brush, transferred though an ascending gradient of PB-based sucrose solutions, and then subjected to a freeze-thaw cycle using liquid nitrogen. The biocytin label was revealed using a Vectastein Elite ABC kit (Axxora, Grünberg, Germany) and 3,3-diaminobenzidenetetrahydrochloride (DAB) histology. Briefly, slices were incubated in ABC solution overnight before the peroxidase reaction end product was revealed by DAB. To enhance the contrast for the EM, the slices were briefly treated with osmium tetroxide solution (4%), followed by an uranylacetate (1%) containing ethanol solution (%70) for dehydration. The slices were embedded in epon resin (Fluka, Switzerland). Sections were prepared for light microscopy and regions of interest were then observed under transmission EM (see Anderson et al. [1994] for details). Briefly, serial ultrathin sections were collected at 60 nm thickness on Pioloform-coated single-slot copper grids (Bio-Rad, Hempstead, England). Labeled spines were photographed at a magnification of 25,000×. Digitized images were processed using the Reconstruct program (John C. Fiala, Boston University) to outline the labeled structures for 3D reconstructions.

SUPPLEMENTAL DATA

The Supplemental Data include three figures, two tables, and Supplemental Experimental Procedures and can be found with this article online at http://www.neuron.org/supplemental/S0896-6273(08)00766-6.

ACKNOWLEDGMENTS

The authors acknowledge the collaboration of the BIZ (Ludwig-Maximilians University Munich) and TILL Photonics GmbH and support from the Boehringer Ingelheim Fonds (N.B.), the National Research Council of Portugal (R.F.), the Alexander von Humboldt Stiftung, and a Marie Curie European fellowship (C.J.W.). We thank C. Huber, N. Stöhr, F. Voss, and M. Braun for technical assistance, R. Bopp for the electronmicroscopy (in the lab of K.A.C. Martin, ETH Zürich, supported by SNF NCCR 'Neural Plasticity and Repair'), and T. Keck, T. Mrsic-Flögel, and V. Scheuss for comments on the manuscript.

Accepted: September 3, 2008
Published: November 25, 2008

REFERENCES

Anderson, J.C., Douglas, R.J., Martin, K.A., and Nelson, J.C. (1994). Map of the synapses formed with the dendrites of spiny stellate neurons of cat visual cortex. J. Comp. Neurol. *341*, 25–38.

Arellano, J.I., Espinosa, A., Fairen, A., Yuste, R., and Defelipe, J. (2007). Non-synaptic dendritic spines in neocortex. Neuroscience *145*, 464–469.

Bastrikova, N., Gardner, G.A., Reece, J.M., Jeromin, A., and Dudek, S.M. (2008). Synapse elimination accompanies functional plasticity in hippocampal neurons. Proc. Natl. Acad. Sci. USA *105*, 3123–3127.

Darcy, K.J., Staras, K., Collinson, L.M., and Goda, Y. (2006). Constitutive sharing of recycling synaptic vesicles between presynaptic boutons. Nat. Neurosci. *9*, 315–321.

De Paola, V., Arber, S., and Caroni, P. (2003). AMPA receptors regulate dynamic equilibrium of presynaptic terminals in mature hippocampal networks. Nat. Neurosci. *6*, 491–500.

De Paola, V., Holtmaat, A., Knott, G., Song, S., Wilbrecht, L., Caroni, P., and Svoboda, K. (2006). Cell type-specific structural plasticity of axonal branches and boutons in the adult neocortex. Neuron *49*, 861–875.

Deng, J., and Dunaevsky, A. (2005). Dynamics of dendritic spines and their afferent terminals: spines are more motile than presynaptic boutons. Dev. Biol. *277*, 366–377.

Dudek, S.M., and Bear, M.F. (1992). Homosynaptic long-term depression in area CA1 of hippocampus and effects of N-methyl-D-aspartate receptor blockade. Proc. Natl. Acad. Sci. USA *89*, 4363–4367.

Engert, F., and Bonhoeffer, T. (1999). Dendritic spine changes associated with hippocampal long-term synaptic plasticity. Nature *399*, 66–70.

Gähwiler, B.H. (1981). Organotypic monolayer cultures of nervous tissue. J. Neurosci. Methods *4*, 329–342.

Garner, C.C., Nash, J., and Huganir, R.L. (2000). PDZ domains in synapse assembly and signalling. Trends Cell Biol. *10*, 274–280.

Harris, K.M., and Stevens, J.K. (1989). Dendritic spines of CA 1 pyramidal cells in the rat hippocampus: serial electron microscopy with reference to their biophysical characteristics. J. Neurosci. *9*, 2982–2997.

Knott, G.W., Holtmaat, A., Wilbrecht, L., Welker, E., and Svoboda, K. (2006). Spine growth precedes synapse formation in the adult neocortex in vivo. Nat. Neurosci. *9*, 1117–1124.

Konur, S., and Yuste, R. (2004). Imaging the motility of dendritic protrusions and axon terminals: roles in axon sampling and synaptic competition. Mol. Cell. Neurosci. *27*, 427–440.

Krueger, S.R., Kolar, A., and Fitzsimonds, R.M. (2003). The presynaptic release apparatus is functional in the absence of dendritic contact and highly mobile within isolated axons. Neuron *40*, 945–957.

Lang, C., Barco, A., Zablow, L., Kandel, E.R., Siegelbaum, S.A., and Zakharenko, S.S. (2004). Transient expansion of synaptically connected dendritic spines upon induction of hippocampal long-term potentiation. Proc. Natl. Acad. Sci. USA *101*, 16665–16670.

Maletic-Savatic, M., Malinow, R., and Svoboda, K. (1999). Rapid dendritic morphogenesis in CA1 hippocampal dendrites induced by synaptic activity. Science *283*, 1923–1927.

Matsuzaki, M., Honkura, N., Ellis-Davies, G.C., and Kasai, H. (2004). Structural basis of long-term potentiation in single dendritic spines. Nature *429*, 761–766.

Nägerl, U.V., Eberhorn, N., Cambridge, S.B., and Bonhoeffer, T. (2004). Bidirectional activity-dependent morphological plasticity in hippocampal neurons. Neuron *44*, 759–767.

Nägerl, U.V., Köstinger, G., Anderson, J.C., Martin, K.A.C., and Bonhoeffer, T. (2007). Protracted synaptogenesis after activity-dependent spinogenesis in hippocampal neurons. J. Neurosci. *27*, 8149–8156.

Schikorski, T., and Stevens, C.F. (1997). Quantitative ultrastructural analysis of hippocampal excitatory synapses. J. Neurosci. *17*, 5858–5867.

Stettler, D.D., Yamahachi, H., Li, W., Denk, W., and Gilbert, C.D. (2006). Axons and synaptic boutons are highly dynamic in adult visual cortex. Neuron *49*, 877–887.

Toni, N., Buchs, P.A., Nikonenko, I., Bron, C.R., and Muller, D. (1999). LTP promotes formation of multiple spine synapses between a single axon terminal and a dendrite. Nature *402*, 421–425.

Tsuriel, S., Geva, R., Zamorano, P., Dresbach, T., Boeckers, T., Gundelfinger, E.D., Garner, C.C., and Ziv, N.E. (2006). Local sharing as a predominant determinant of synaptic matrix molecular dynamics. PLoS Biol. *4*, e271. 10.1371/journal.pbio.0040271.

Umeda, T., Ebihara, T., and Okabe, S. (2005). Simultaneous observation of stably associated presynaptic varicosities and postsynaptic spines: morphological alterations of CA3–CA1 synapses in hippocampal slice cultures. Mol. Cell. Neurosci. *28*, 264–274.

Vanden Berghe, P., and Klingauf, J. (2006). Synaptic vesicles in rat hippocampal boutons recycle to different pools in a use-dependent fashion. J. Physiol. *572*, 707–720.

Waters, J., and Smith, S.J. (2002). Vesicle pool partitioning influences presynaptic diversity and weighting in rat hippocampal synapses. J. Physiol. *541*, 811–823.

Yao, J., Qi, J., and Chen, G. (2006). Actin-dependent activation of presynaptic silent synapses contributes to long-term synaptic plasticity in developing hippocampal neurons. J. Neurosci. *26*, 8137–8147.

Yuste, R., and Bonhoeffer, T. (2001). Morphological changes in dendritic spines associated with long-term synaptic plasticity. Annu. Rev. Neurosci. *24*, 1071–1089.

Yuste, R., and Bonhoeffer, T. (2004). Genesis of dendritic spines: insights from ultrastructural and imaging studies. Nat. Rev. Neurosci. *5*, 24–34.

Zhou, Q., Homma, K.J., and Poo, M.M. (2004). Shrinkage of dendritic spines associated with long-term depression of hippocampal synapses. Neuron *44*, 749–757.